FORWARD NEUTRON AND PHOTON RESULTS FROM HERA

Armen Bunyatyan

for the H1 and ZEUS Collaborations

DESY, Notkestrasse 85, Hamburg, Germany
E-mail: armen.bunyatyan@desy.de

Recent measurements of the forward neutron and forward photon production in deep-inelastic scattering obtained by the H1 and ZEUS Collaborations are presented. Results are compared with different Monte Carlo models which are commonly used for simulations of deep-inelastic scattering processes and cosmic ray air showers.

1 Introduction

Particle production at very small angles with respect to the proton beam direction *(forward direction)* in a process with a hard scale provides a testing ground for the theory of strong interactions in the soft regime and is important for the theoretical understanding of proton fragmentation. Measurements of forward particles also provide important constraints for the modelling of the high energy air showers and thereby are very valuable for the understanding of high energy cosmic ray data [1]. Here the recent results of the H1 and ZEUS Collaborations of the forward neutron and photon production in electron-proton and positron-proton interactions at HERA collider are reported.

2 Forward neutrons in DIS and in the photoproduction of dijets

The measurements of events with neutrons carrying a large fraction x_L of the incident proton beam energy in ep scattering at HERA [2]-[9] has led to renewed interest in the QCD evolution and factorisation properties of proton fragmentation to leading neutrons (LN). The process leading to such events, $ep \to e'nX$, is illustrated in Fig. 1a. Although a fraction of these LNs may result from the hadronisation of the proton remnant, the

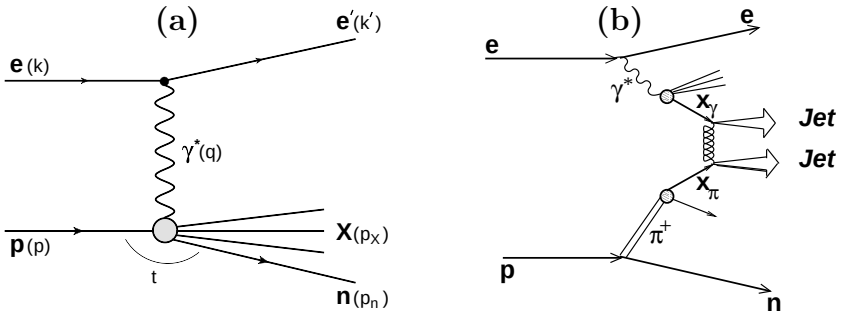

Figure 1: (a) Generic diagram for leading neutron production $ep \to e'nX$ in deep-inelastic scattering. (b) A diagram for the dijet production process $ep \to e' + n + jet + jet + X$ assuming this proceeds via pion exchange.

t-channel exchange of colour singlet virtual particles like the one illustrated in Fig. 1b is expected to contribute significantly [10]-[14]. In this picture, the proton fluctuates into a a state consisting of a positively charged pion and a neutron $p \to n\pi^+$; the virtual photon subsequently interacts with a parton from the pion, leaving a fast forward neutron in the final state. In the simple exchange picture, the cross section factorises into two parts: one factor describes the proton fluctuation into a $n\pi^+$ state, the other describes the photon-pion scattering, so that the LN production is largely independent of the variables describing the photon vertex *(vertex factorisation)*. The cross section can be written as $d\sigma_{\gamma^* p \to nx} = f_{\pi/p}(x_L, t) \times d\sigma_{\gamma^* \pi \to X}$. Here $f_{\pi/p}$ is the flux of virtual pions in the proton, a factor constrained from low energy hadronic data; $x_L \approx E_n/E_p$ is the neutron longitudinal momentum fraction and t is the four-momentum transfer squared at the proton vertex.

The H1 and ZEUS experiments measured the LN production in deep-inelastic scattering (DIS) and photoproduction events. These neutrons were measured with lead-scintillator forward calorimeters (FNC), situated at a zero degree polar angle at 106 m from the H1 and ZEUS interaction points, after the proton beam was bent vertically; magnet apertures limited neutron detection to scattering angles less than 0.75 mrad.

Figure 2 shows the cross sections of LN production as a function of x_L in DIS [8], in the phase space defined by the photon virtuality 6 GeV^2 $< Q^2 <$ 100 GeV^2 and the inelasticity $0.02 < y < 0.6$, and in the photoproduction of dijets [7], in the kinematic range defined by $Q^2 < 1$ GeV^2 and the jet transverse energies and pseudorapidities $E_T^{jet1(2)} > 7.5$ (6.5)GeV, $-1.5 < \eta^{jet1,2} < 2.5$. The measurements are compared with

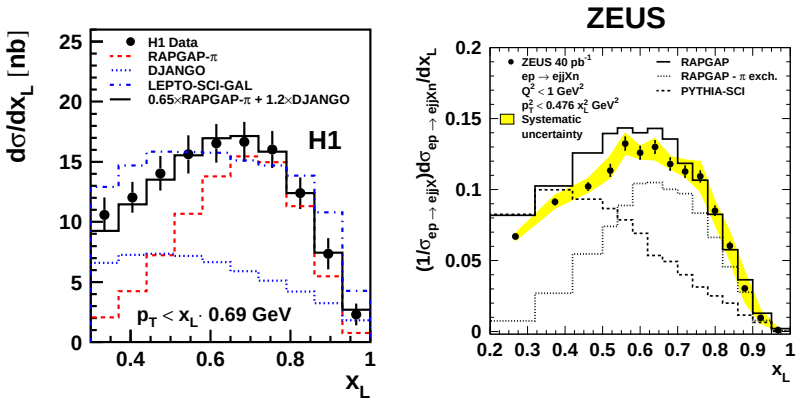

Figure 2: Differential cross section of forward neutron production as a function of x_L in the angular range $\theta_n < 0.75$ mrad in DIS (left) and in the photoproduction of dijets (right). Predictions of the MC simulations are compared to the measurements.

the Monte Carlo (MC) simulations. The DIS measurement is compared with the prediction of RAPGAP MC [16], which generates exclusively the π^+-exchange process, and the standard fragmentation model simulated with DJANGOH MC [15]. For the comparison with the photoproduction data, the RAPGAP simulation incorporates the standard fragmentation and the π^+-exchange processes. The photoproduction measurement is also compared with the PYTHIA MC, which includes the simulation of soft colour interactions (SCI) [17], in which the production of diffraction-like configurations is enhanced via non-perturbative colour rearrangements between the outgoing partons. Both distributions are well described by the combination of the standard fragmentation and π^+-exchange models. At large x_L values the contribution from π^+-exchange dominates.

2.1 Leading Neutron x_L and p_T^2 cross sections in DIS

The measurement of the double differential cross sections of LN production in DIS as function of x_L and the neutron transverse momentum squared p_T^2 [9] is shown in the left side of Fig. 3. The best description of the data is achieved by the combination of the standard fragmentation and π^+-exchange models, similar to the single differential x_L distribution shown in the left side of Fig.2. Assuming vertex factorisation the p_T^2

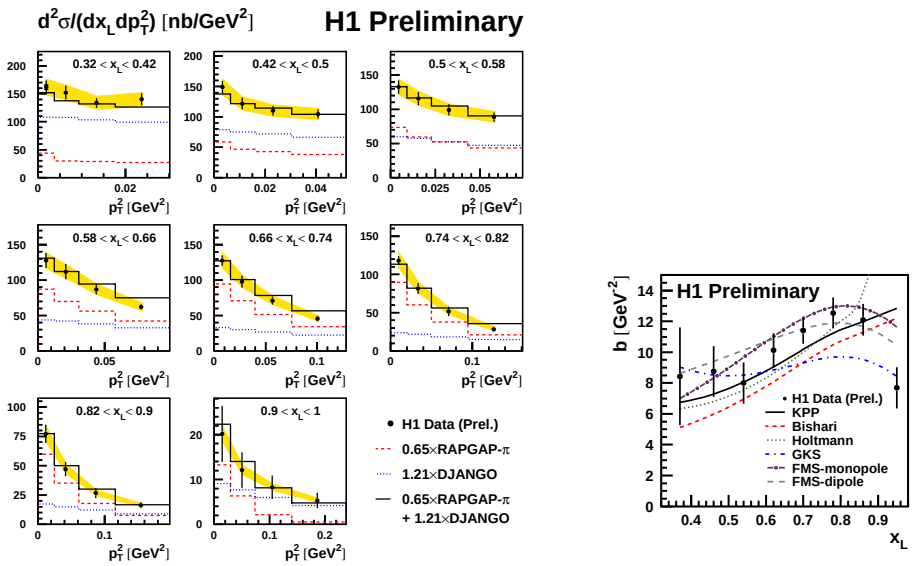

Figure 3: (Left) Double differential cross section of forward neutron production as a function of p_T^2 and x_L of the neutron. Data are compared with predictions of the RAPGAP pion exchange and DJANGOH MC simulations as well as combination of those two simulations. (Right) b-slopes of the p_T^2 distributions of forward neutrons compared with different pion flux parameterisations.

distribution is directly related to the pion flux. The p_T^2 distributions can be fitted by an exponential function $a(x_L)\exp\left(-b(x_L)p_T^2\right)$ in each x_L bin. The obtained values of the p_T^2 slopes (parameter $b(x_L)$) are shown in the right side of Fig. 3 together with the several parameterisations of the pion flux. Most of the shown predictions describe the data within uncertainties.

2.2 Photoproduction of dijets with LN

The dijet photoproduction cross sections in events with and without the LN requirement are measured for jets in the phase space described in section 2 [7]. The fraction of dijet events which contain a LN in the measured kinematic region is $6.63 \pm 0.07(\text{stat.}) \pm 0.20(\text{syst.})\%$. The differential cross sections as functions of the event variables x_γ^{OBS},

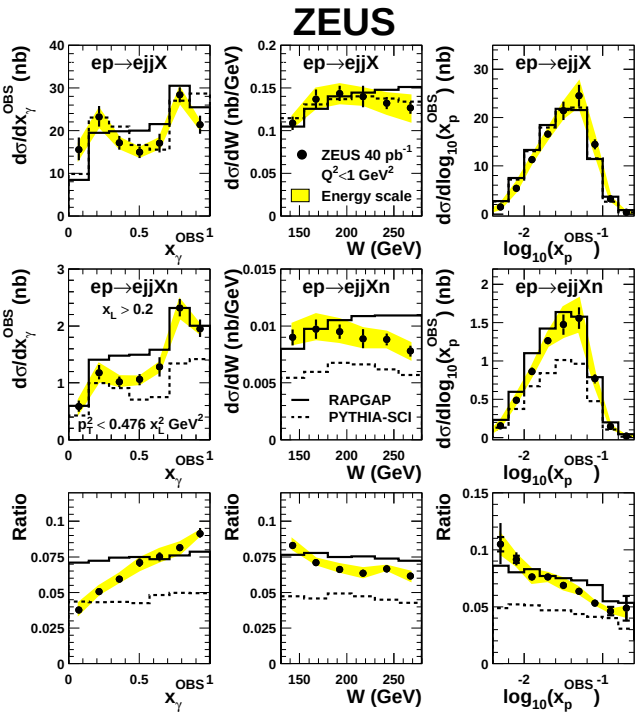

Figure 4: Differential cross sections of dijet photoproduction with leading neutrons and inclusive dijet photoproduction as functions of x_γ^{OBS}, W and $\log_{10}(x_p^{OBS})$. The ratios between cross sections are also given.

x_p^{OBS} and W are presented in Figure 4. Here, x_γ^{OBS} and x_p^{OBS} are respectively the fractions of the four-momenta of the photon and the proton which participate in the hard interaction and W is the centre-of-mass energy of the γp system. The LN sample has a significantly smaller contribution at low x_γ^{OBS}. The cross sections are roughly flat as a function of W; the yield exhibits a decrease with increasing W and x_p^{OBS}. For the LN sample, RAPGAP overestimates the cross section at low x_γ^{OBS} while PYTHIA-SCI underestimates the cross section at high x_γ^{OBS}. Neither model can reproduce the dependence of the neutron yield on x_γ^{OBS} and W. The RAPGAP model predicts a small decrease of the neutron yield with x_p^{OBS}, which however is less pronounced than in the data. This dependence of the neutron yield indicates a violation of vertex factorisation.

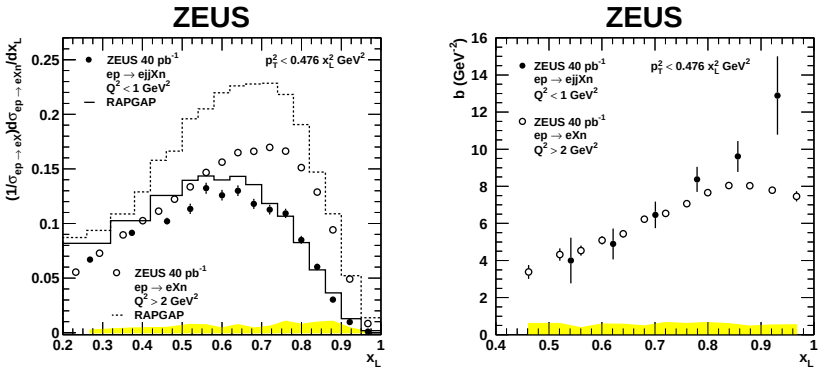

Figure 5: (left) Differential cross sections as a function of x_L for dijet photoproduction and for DIS. Both distributions are normalised by their respective cross sections without requirement of LN. (right) Exponential slopes b versus x_L from fits of the p_T^2 distributions. The solid points are for dijet photoproduction, the open points for DIS.

2.3 Comparison of LN production in DIS and in the dijet photoproduction

The left side of Figure 5 presents the normalised x_L distribution of LN in dijet photoproduction [7] and in inclusive DIS with $Q^2 > 2$ GeV^2 [6]. The yield of neutrons from dijet photoproduction agrees with that in DIS at low $x_L < 0.4$, but is lower at higher x_L. For $x_L > 0.8$ the yield in dijet photoproduction is more than a factor of two lower than in inclusive DIS. The RAPGAP MC predicts the shapes of distributions fairly well. After normalising each prediction to its respective data set RAPGAP provides a fair description of the drop of the neutron yield with x_L in dijet photoproduction relative to that in DIS. The right side of Figure 5 shows the exponential p_T^2 slopes $b(x_L)$ for dijet photoproduction and inclusive DIS. They are similar in magnitude and both rise with x_L. Although the slopes rise somewhat faster with x_L in the dijet photoproduction data, there is no statistically significant difference between the two sets except for $x_L > 0.9$.

3 Forward photon spectra in DIS

The production of photons at very small angles with respect to the proton beam direction is studied in DIS at HERA [18] by the H1 Experiment. The analysis covers the kinematic

range of 6 GeV^2 $< Q^2 <$ 100 GeV^2 and $0.05 < y < 0.6$. The forward photons are measured in the FNC calorimeter.

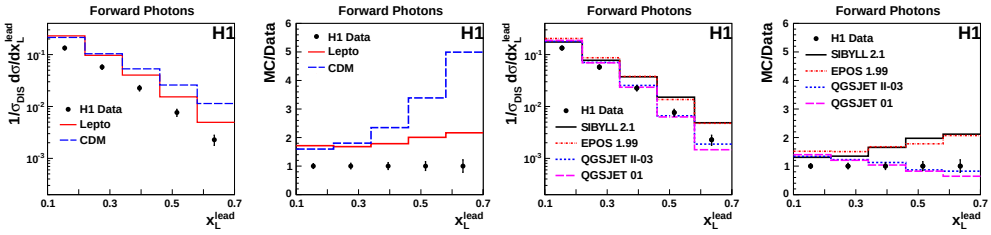

Figure 6: The normalised cross sections for the production of forward photons in the pseudorapidity range $\eta > 7.9$ in DIS in the kinematic region $6 < Q^2 < 100$ GeV^2 and $0.05 < y < 0.6$ as a function of the longitudinal momentum fraction x_L^{lead} of the leading photon.

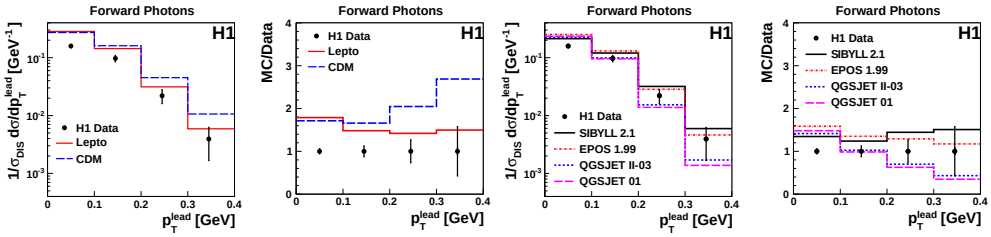

Figure 7: The normalised cross sections for the production of forward photons in the pseudorapidity range $\eta > 7.9$ in DIS in the kinematic region $6 < Q^2 < 100$ GeV^2 and $0.05 < y < 0.6$ as a function of the transverse momentum of the leading photon p_T^{lead}.

For the most energetic forward photon in the pseudorapidity range $\eta > 7.9$ the cross sections are presented as a function of its transverse momentum p_T^{lead} and longitudinal momentum fraction of the incoming proton x_L^{lead} (Figures 6-7). The data are compared with DJANGOH [15] MC model predictions, in which higher order QCD effects are simulated using leading log parton showers as implemented in LEPTO [19], or using the Colour Dipole Model (CDM) as implemented in ARIADNE [20]. The measurements are also compared with the predictions of several hadronic interaction models which are commonly used for the simulation of cosmic ray air shower cascades: EPOS [21],

QGSJET 01 [22], QGSJET II-03 [23] and SIBYLL [24]. The ratios of the MC predictions to the measured cross sections are also shown.

All models overestimate the total rate of forward photons. The shapes of measured distributions are well described by LEPTO. CDM predicts harder x_L and p_T spectra. The QGSJET models predict slightly softer spectra. The EPOS and SIBYLL models predict harder x_L spectra, but reasonably describe the shape of p_T distribution.

4 Summary

The production of leading neutrons has been studied in DIS and in the photoproduction of dijets. The contributions from fragmentation processes and from the exchange of colour-neutral particles such as π^+ are required to describe the LN data. The p_T^2 spectra of forward neutrons show sensitivity to the pion flux parameterisations.

The production of forward photons has been studied in DIS as a function of the longitudinal momentum fraction x_L and the transverse momentum p_T. Predictions of Monte Carlo models overestimate the rate of forward photon production. All these models predict different spectra in x_L and p_T; none of them can describe the photon data in rate and in shape.

The present measurements may lead to further understanding of proton fragmentation in collider and cosmic ray experiments.

Acknowledgements

I wish to thank the organisers for this interesting, stimulating and enjoyable conference.

References

[1] A. Bunyatyan *et al.*, Proceedings of the Workshop on the Implications of HERA for LHC Physics, 26-30 May 2008, p.611, DESY-PROC-2009-02 [arXiv:0903.3861].

[2] C. Adloff *et al.* [H1 Coll.], Eur. Phys. J. C **6** (1999) 587 [hep-ex/9811013].

[3] S. Chekanov *et al.* [ZEUS Coll.], Nucl. Phys. B **637** (2002) 3 [hep-ex/0205076].

[4] A. Aktas *et al.* [H1 Coll.], Eur. Phys. J. C **41** (2005) 273 [hep-ex/0501074].

[5] S. Chekanov *et al.* [ZEUS Coll.], Phys. Lett. B **590** (2004) 143 [hep-ex/0401017].

[6] S. Chekanov *et al.* [ZEUS Coll.], Nucl. Phys. B **776** (2007) 1 [hep-ex/0702028].

[7] S. Chekanov *et al.* [ZEUS Coll.], Nucl. Phys. B **827** (2010) 1 [arXiv:0909.3032].

[8] F. D. Aaron *et al.* [H1 Coll.], *Eur. Phys. J.* **C68** (2010) 381 [arXiv:1001.0532].

[9] H1 Collaboration, *Leading Neutron p_T distributions*, H1prelim-10-113, *http://www-h1.desy.de/h1/www/publications/htmlsplit/H1prelim-10-113.long.html*.

[10] J.D. Sullivan, Phys. Rev. D **5** (1972) 1732.

[11] M. Bishari, Phys. Lett. B **38** (1972) 510.

[12] H. Holtmann *et al.*, Phys. Lett. B **338** (1994) 363.

[13] B. Kopeliovich, B. Povh and I. Potashnikova, Z. Phys. C **73** (1996) 125 [hep-ph/9601291].

[14] M. Przybycień, A. Szczurek and G. Ingelman, Z. Phys. C **74** (1997) 509 [hep-ph/9606294].

[15] K. Charchula, G. A. Schuler and H. Spiesberger, DJANGOH 1.4, *Comput. Phys. Commun.* **81**, 381 (1994).

[16] H. Jung, RAPGAP 3.1, *Comp. Phys. Commun.* **86** (1995) 147.

[17] A. Edin, G. Ingelman and J. Rathsman, Phys. Lett. **B366** (1996) 371 [hep-ph/9508386].

[18] F. D. Aaron *et al.* [H1 Coll.], DESY-11-093 [arXiv:1106.5944].

[19] G. Ingelman, A. Edin and J. Rathsman, LEPTO 6.5, *Comput. Phys. Commun.* **101** (1997) 108 [hep-ph/9605286].

[20] L. Lönnblad, ARIADNE 4.10, *Comput. Phys. Commun.* **71** (1992) 15.

[21] K. Werner, F.-M. Liu and T. Pierog, *Phys. Rev.* **C74** (2006) 044902 [hep-ph/0506232].

[22] N. Kalmykov, S. Ostapchenko, A. Pavlov, *Nucl.Phys. Proc. Suppl.* **52B** (1997) 17.

[23] S. Ostapchenko, *AIP Conf. Proc.* **928** (2007) 118 [arXiv:0706.3784].

[24] E.-J. Ahn *et al.*, *Phys. Rev.* **D80** (2009) 094003 [arXiv:0906.4113].